Histol Histopathol (2023) 38: 1391-1401

Histology and Histopathology
From Cell Biology to Tissue Engineering

ORIGINAL ARTICLE Open Access

Protein atlas of fibroblast specific protein 1 (FSP1)/S100A4

Bettina Marturet Fendt[1], Astrid Hirschmann[1], Malgorzata Bruns[1], Eva Camarillo-Retamosa[2], Caroline Ospelt[2] and Alexander Vogetseder[1]

[1]Institute of Pathology, Cantonal Hospital Lucerne, Lucerne and [2]Department of Rheumatology, Center of Experimental Rheumatology, University Hospital Zurich, University of Zurich, Zurich, Switzerland

Summary. Fibroblast specific protein 1 (FSP1)/S100A4 is a calcium binding protein which has been linked to epithelial-mesenchymal transition, tissue fibrosis, pulmonary vascular disease, metastatic tumour development, increased tumour cell motility and invasiveness. This protein is reported to be also expressed in newly formed and differentiated fibroblasts and has been used in various studies to demonstrate epithelial-mesenchymal transition (EMT).

We aimed to characterize S100A4 positive cells in different human tissue compartments, with the focus on fibroblasts/myofibroblast.

We found S100A4 expression in a wide range of cells. Fibroblasts/myofibroblasts showed a broad spectrum of staining intensity, ranging from negative to strong expression of S100A4, with the strongest expression in smooth muscle actin positive myofibroblasts. Cells of haematopoietic lineage, namely CD4 and CD8 positive T-lymphocytes, but not B-lymphocytes expressed S100A4. All investigated monocytes, macrophages and specialised histiocytes were positive for S100A4. Even some epithelial cells of the kidney and bladder were positive for S100A4. Expression was also found in the vasculature. Here, cells of the subendothelial space, tunica adventitia and some smooth muscle cells of the tunica media were positive for S100A4. In summary, S100A4 is expressed in various cell types of different lineage and is not, as originally believed, specific for fibroblasts (FSP). Results attained under the premise of specificity of FSP1/S100A4 for fibroblasts, like the founding research on EMT type 2 in kidney and liver, therefore need to be reinterpreted.

Key words: FSP1, S100A4, EMT, Protein atlas

Corresponding Author: Bettina Marturet Fendt, Institute of Pathology, Cantonal Hospital Lucerne, Lucerne, Switzerland. e-mail: bettina.fendt@luks.ch

www.hh.um.es. DOI: 10.14670/HH-18-621

Introduction

Fibroblast specific protein (FSP1/S100A4) is an intracellular calcium binding protein localized in the cytoplasm and/or nucleus that regulates several cellular processes.

It can bind to intracellular target proteins, including actins, non-muscle myosin IIA, tropomyosin and liprin-β1 to form complexes that regulate cell motility (Fei et al., 2017) and is expressed in highly motile cells like macrophages. Similarly, S100A4 is reported to be linked to increased tumour cell motility, invasiveness and metastatic tumour development (Sherbet, 2009). Further, it has oncogenic properties by inhibiting p53-dependent processes like cycle arrest and apoptosis by degrading p53 (Orre et al., 2013). Recent data also shows an extracellular function of S100A4. S100A4 is secreted in response to various stimuli such as activated normal T cell expressed and secreted factors (RANTES) produced by the tumor cells and plays a role in extracellular matrix (ECM) remodeling and angiogenesis (Li et al., 2020).

This protein, as the name implies, was originally believed to be solely expressed in fibroblasts/myofibroblasts and its appearance was linked to epithelial-mesenchymal transition (EMT). EMT is the phenotypic transition of epithelial cells to mesenchymal lineage with cells losing their epithelial characteristics and acquiring mesenchymal features. EMT is subdivided into 3 subtypes (Kalluri and Weinberg, 2009). Type 1 EMT is associated with implantation and embryonic gastrulation and gives rise to mesoderm and endoderm as well as mobile neural crest cells. The primitive

Abbreviations. ACR/EULAR, American College of Rheumatology/European League Against Rheumatism; ATP, Adenosine triphosphate; DAPI, 4′,6-diamidino-2-phenylindole; DMEM, Dulbecco's modified Eagle's medium; EMT, Epithelial-mesenchymal transition; FCS, Fetal calf serum; FITC, Fluorescein isothyocyanate; FSP1, Fibroblast specific protein 1; IF, Immunofluorescence; MET, Mesenchymal-epithelial transition; TMA, Tissue microarrays; PBMC, Peripheral blood mononuclear cells; RA, Rheumatoid arthritis

epithelium, specifically the epiblast, gives rise to primary mesenchyme via EMT. This primary mesenchyme can be reinduced to form secondary epithelia by mesenchymal-epithelial transition (MET). It is speculated that such secondary epithelia may further differentiate to form other types of epithelial tissues, undergoing subsequent EMT to generate the cells of connective tissue, including astrocytes, adipocytes, chondrocytes, osteoblasts, and muscle cells (Kalluri and Weinberg, 2009; Thiery et al., 2009).

Type 2 EMT refers to the transition of specialised secondary epithelial cells (e.g., proximal tubular cells in the kidney) into myofibroblasts with substantial pro-fibrotic and pro-inflammatory activity. Proposed steps in type 2 EMT are the loss of cell-cell contact and apical-basal polarity besides cellular destabilisation with reduction of E-cadherin and zonula occludens. In the intermediate phase, both epithelial and mesenchymal markers are expressed, matrix metalloproteinases (especially MMP2 and MMP9) are up regulated and MMP-inhibitors are down regulated, leading to disruption of underlying basement membranes. Finally, there is a transition to mesenchymal phenotype with the formation of the enlarged spindle-shaped myofibroblast (Burns and Thomas, 2010).

Type 3 EMT represents an important stage of the evolution of epithelial cancers that leads to a more aggressive phenotype associated with uncontrolled growth, migration and invasion (sarcomatous growth) (Saitoh, 2018).

The first study using a FSP1/S100A4 antibody to demonstrate EMT type 2 was published in 1995 (Strutz et al., 1995) and laid the foundation for the hypothesis of type 2 EMT. Based on their investigations using subtractive and differential hybridization for transcript comparison between murine fibroblasts and isogenic epithelium, the authors reported that FSP1 is relatively specific for fibroblasts. Using a mouse model of renal interstitial fibrosis with persistent interstitial inflammation, they hypothesized that fibroblasts in some cases arise from kidney epithelium. Additionally, the in vitro overexpression of FSP1 cDNA in tubular epithelium was accompanied by conversion to a mesenchymal phenotype. Finally, results of experiments with a tubular mouse epithelium cell line submerged in type I collagen gels, led to the generation of the type 2 EMT hypothesis.

In subsequent years, this hypothesis was tested by employing antibodies directed against FSP1 in other organs such as the liver. These results indicated that adult mouse hepatocytes undergo phenotypic and functional changes typical of epithelial to mesenchymal transition. Additionally, it was reported that hepatocytes, which undergo EMT, contribute substantially to the population of FSP1-positive fibroblasts in liver fibrosis (Zeisberg et al., 2007).

After the establishment of the EMT type 2 concept, many scientific papers have been published that employed a FSP1/S100A4 antibody to demonstrate EMT (Hertig et al., 2006; Kutlu and Alcigir, 2019).

In recent years, the specificity of FSP1/S100A for fibroblasts has been questioned (Le Hir et al., 2005; Koesters et al., 2010). Since the EMT type 2 theory is based on cells expressing FSP1 (Strutz et al., 1995), we set out to characterise and catalogue cells that express S100A4 in different human tissues, with special emphasis on fibroblasts/myofibroblasts in different functional states.

Materials and methods

Tissue

Non-malignant paraffin-embedded human tissue samples were retrieved from the pathology archive of the Lucerne cantonal hospital. Sections of 2µm thickness were prepared from soft tissues of different locations and various organs. Primarily sections of a single location were stained but also tissue microarrays (TMA) were employed. These hold multiple human tissue samples in one paraffin block.

Immunohistochemistry/-fluorescence

Immunohistochemical staining was performed on a Leica BOND-III Fully Automated IHC and ISH Staining System (Leica Biosystems), using the Polymer Refine Detection Kit (Leica DS9800). BOND Epitope Retrieval Solution 2 (Leica AR9640) was employed for epitope retrieval. This is a ready to use EDTA based pH 9 epitope retrieval solution for the heat-induced epitope retrieval (HIER) of formalin-fixed, paraffin-embedded tissue.

To avoid nonspecific immunohistochemical staining, 3 different antibodies directed against S100A4 were used in the study. These were obtained from different firms and were generated in different animals (mouse and rabbit). The staining patterns were identical. The S100A4 antibody from Sigma (HPA007973) was used to generate the images shown in this publication. The following antibodies were employed:

CD3 (Agilent Technologies; A045201), dilution 1:200. CD4 (Novocastra; NCL-L-CD4-368), dilution 1:200. CD8 (BioSB; BSB5173), dilution 1:300. CD14 (Abcam; 1H5D8) dilution 1:500. CD45 (Cell Marque; 145M95), dilution 1:400. CD68 (Agilent Technologies ; M087601), dilution 1:200. MART-1/Tyrosinase (BioCare medical; CM 178 A), dilution 1:300. S100 (Agilent Technologies; Z031129), dilution 1:2000. S100A4 (Sigma; Rabbit polyclonal HPA007973), dilution 1:2000. S100A4 (Abcam; Rabbit monoclonal EPR14639(2)), dilution 1:5000. S100A4 (ThermoFisher; Mouse monoclonal CL0239), dilution 1:100. Smooth muscle actin (Cell Marque; 202M-95), dilution 1:300.

For Immunofluorescence, binding sites of the primary antibodies were revealed with Cy3-conjugated goat-anti-rabbit IgG (red) and fluorescein isothyocyanate (FITC)-conjugated goat-anti-mouse IgG (Jackson ImmunoResearch Laboratories, West Grove, PA),

respectively. For nuclear staining, 4′,6-diamidino-2-phenylindole (DAPI; Sigma) was added. Fluorescent-labeled specimens were examined using a confocal laser scanning microscope (CLSM SP2, Leica, Mannheim, Germany) or a Polyvar microscope (Reichert Jung, Vienna, Austria).

Cell culture

Synovial tissues were obtained from rheumatoid arthritis (RA) patients undergoing joint replacement surgery at the Schulthess Clinic Zurich, Switzerland. RA patients fulfilled the 2010 ACR/EULAR (American

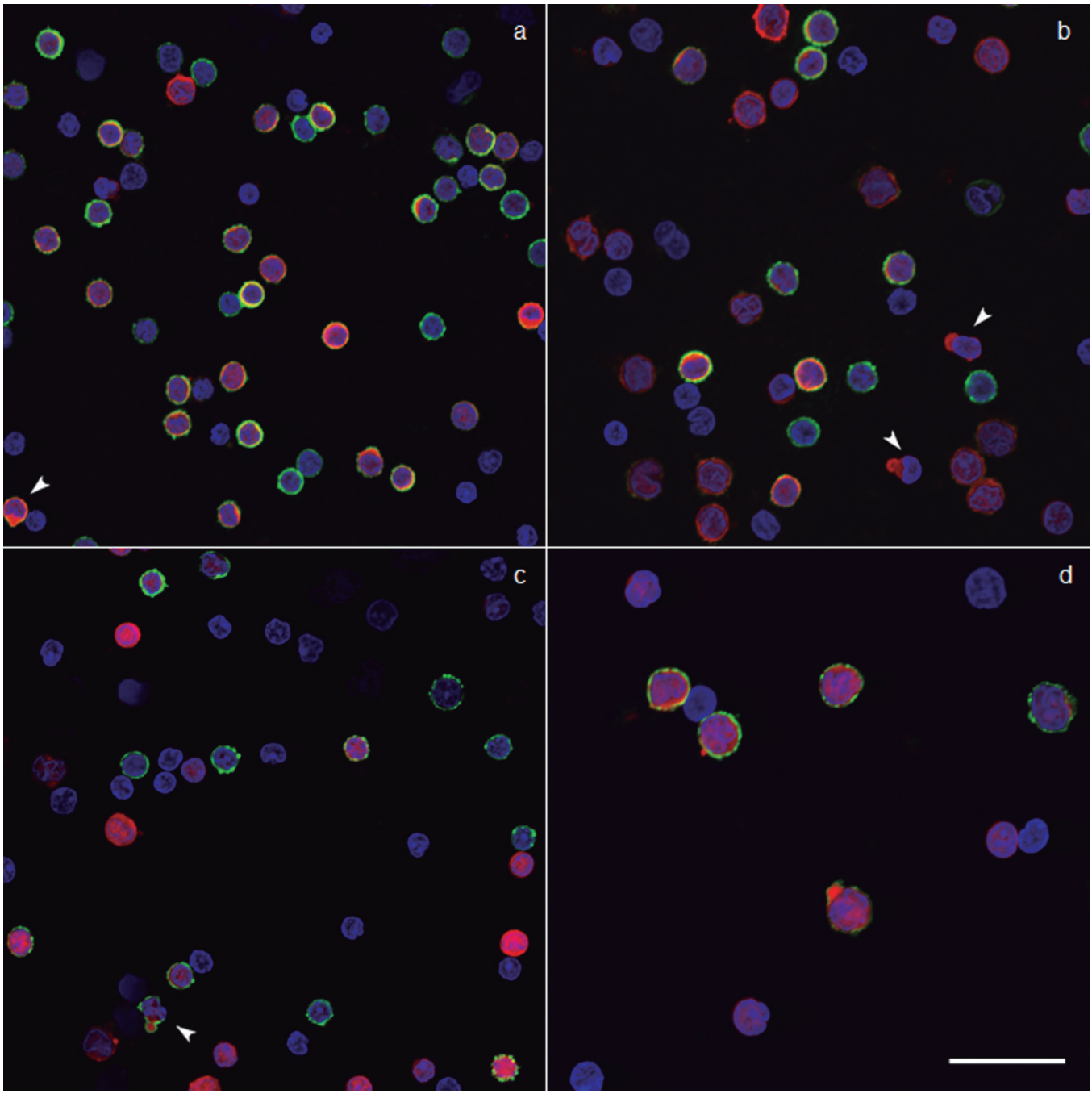

Fig. 1. Isolated leukocytes co-stained with various leucocyte markers and FSP1/S100A4, then visualized by immunofluorescence (IF) staining. **a.** Co-staining of CD3 (green) and S100A4 (red). **b.** Co-staining of CD4 (green) and S100A4 (red). **c.** Co-staining of CD8 (green) and S100A4 (red). **d.** Co-staining of CD14 (green) and FSP1/S100A4 (red). DAPI stain (blue). Arrowheads: mature cytotoxic T-cells. Scale bar: 40 μm. a, b, x 500; c, x 550; d, x 600.

College of Rheumatology/European League Against Rheumatism) criteria for the classification of RA. The study was approved by the local ethic committees of the University Hospital Zurich, Switzerland. Informed consent was obtained from all patients. Synovial tissues were digested with dispase (37ºC, 1h) and synovial fibroblasts were cultured in Dulbecco's modified Eagle's medium (DMEM; Life Technologies) supplemented with 10% fetal calf serum (FCS), 50 U ml^{-1} penicillin/streptomycin, 2 mM L-glutamine, 10 mM HEPES and 0.2% amphotericin B (all from Life Technologies). Synovial fibroblasts from passages 5 to 8 were used.

3D micromasses were generated as previously described (Kiener et al., 2010). In brief, synovial fibroblasts were mixed with Matrigel (LDEV-free, Corning) ($3x10^6$ SF/ml Matrigel) and 30 µl droplets added to 12-well plates coated with poly 2-hydroxyethylmethacrylate (Sigma). Micromasses were left in culture for 3 weeks in Dulbecco's modified Eagle's medium (DMEM; Life Technologies) supplemented with 10% fetal calf serum (FCS), 1% penicillin/streptomycin, 1% minimum Essential medium non-Essential Amino Acids (Gibco), 1% ITS + premix (BD) and 8.8 mg/500 ml vitamin C. After 3 weeks, micromasses were fixed with 2% paraformaldehyde. After 24h paraformaldehyde was replaced by 70% ethanol and micromasses were embedded in paraffin and sectioned for IHC.

Isolation of peripheral blood mononuclear cells (PBMCs)

EDTA blood was withdrawn from a healthy volunteer. 30 ml blood was overlaid over 15 ml Ficoll

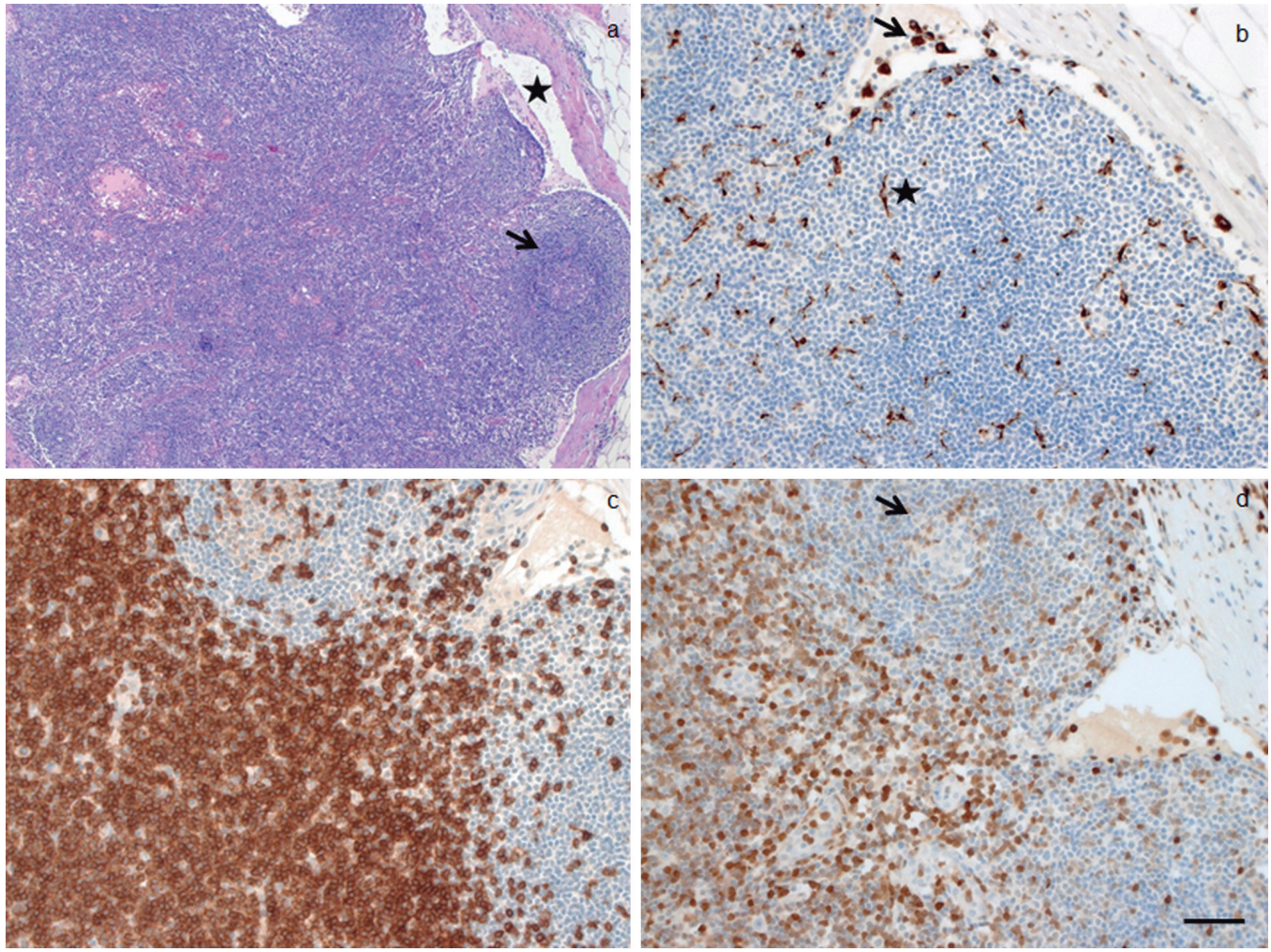

Fig. 2. a. Lymph node showing a secondary lymph follicle (arrow), predominantly composed of B lymphocytes, adjacent to the subcapsular sinus (star); Hematoxylin and eosin stain. **b.** CD68 immunohistochemical staining, positive in dendritic cells (star) and other histiocytes like sinus histiocytes (arrow). **c.** CD3 immunohistochemical staining, positive in CD4+ and CD8+ T-lymphocytes. **d.** S100A4 staining, predominantly positive in the T-cell rich paracortex and predominantly negative in the B-cell rich secondary lymph follicle (arrow). Scale bar: 100 μm. a, x 50; b-d, x 200.

Paque plus at room temperature. The sample was centrifuged for 30 minutes at 450g without breaks. Mononuclear cells from the interface were collected and suspended in PBS. After three additional washing and centrifugation steps, cells were resuspended in an appropriate medium and spun down on histological slides.

Investigated tissues

To investigate tissue rich in fibroblasts and myofibroblasts, we used hypertrophic scar tissue of the skin and palmar fibromatosis. Additionally, human synovial fibroblast cultures (2D and 3D), attained from joints of rheumatoid arthritis patients were stained with S100A4 and smooth muscle actin. Also, fibroblast rich tendon was stained with S100A4.

PBMCs were isolated from peripheral blood and co-stained with S100A4 and different leukocyte markers (CD3, CD4, CD8 and CD14) to exclude a relevant contamination with fibroblasts. CD3 was used as pan-T cell marker, CD4 to identify T-helper cells and CD8 for cytotoxic T-cells. CD14 was used as a marker for monocytes.

Human lymph node was incubated with CD68, CD3 and S100A4. CD68 was used to identify tissue macrophages.

Human kidney, gallbladder, pancreas, oesophagus, colon, stomach, small intestine, liver, thyroid gland, breast, skin, adrenal gland, urinary bladder, prostate, ovary, uterus, skeletal muscle, brain and testis were stained with S100A4 and analysed.

Human skin was additionally stained with CD68 and MART-1 (melanocyte marker).

Connective tissue was incubated with S100A4 and the structures that make up the connective tissue were analysed for S100A4 positivity. These structures included the vasculature, nerve tissue, adipocytes, inflammatory cells and mesenchymal cells of the connective tissue.

Results

In PBMCs, S100A4 was expressed in most CD3+ lymphocytes (Fig. 1a). The analysis showed S100A4 expression in CD4 (Fig. 1b) as well as CD8 positive T-lymphocytes (Fig. 1c). In these cells, S100A4 staining was predominantly cytoplasmic. Also, CD14+ monocytes stained positive for S100A4 (Fig. 1d), displaying a nuclear and cytoplasmic positivity.

In lymph nodes (Fig. 2a), S100A4 staining was observed in areas rich in T cells (Fig. 2c) and in CD68+

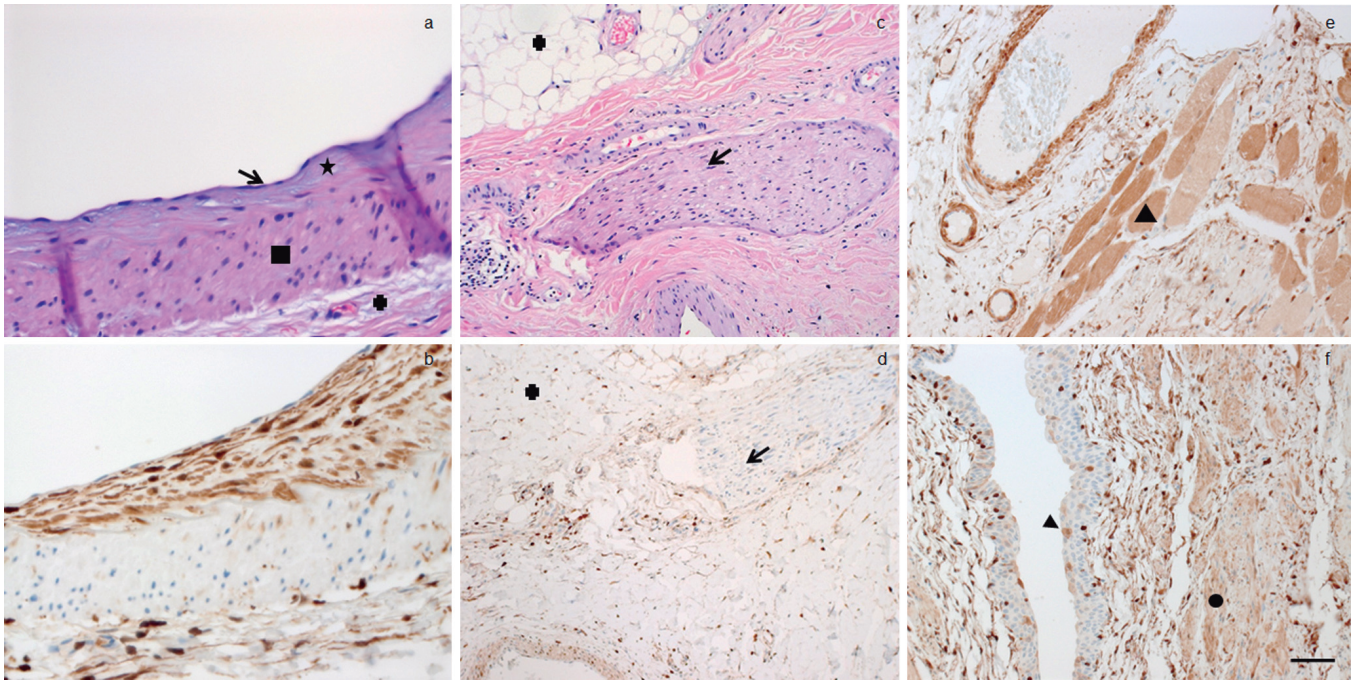

Fig. 3. a. Section of a vessel with endothelium (arrow), subendothelial space (star), tunica media (square) and tunica adventitia (cross); Hematoxylin and eosin stain. **b.** S100A4 staining most of the cells of the subendothelial space, made up of intimal smooth muscle cells and stellate-shaped pericyte-like cells. Some positive cells are seen in the tunica media composed of smooth muscle cells and in the loose connective tissue of the tunica adventitia. **c.** Connective tissue showing a peripheral nerve (arrow) and blood vessels adjacent to adipocytes (cross); Hematoxylin and eosin stain. **d.** S100A4 staining positive in some adipocytes (cross) and negative in a peripheral nerve (arrow). **e.** Skeletal muscle (triangle) with S100A4 positivity (200x). **f.** Urothelial mucosa showing some S100A4 positive umbrella cells (arrowhead) with adjacent smooth muscle layer (circle) with positivity for S100A4. Scale bar: 100 μm. a, b, x 400; c-f, x 200.

histiocytes and dendritic cells (Fig. 2b,d) but not in B cell rich areas (Fig. 2d). In vessels of connective tissue (Fig. 3a,b), S100A4 was highly expressed (nuclear and cytoplasmic) in cells of the subendothelial space, consisting of intimal smooth muscle cells, stellate-shaped pericyte-like cells and in the loose connective tissue of the tunica adventitia. Some positive cells were seen in the tunica media composed of smooth muscle cells, which expressed S100A4 in the cytoplasm. S100A4 was also expressed in the nuclei of most adipocytes of connective tissue (Fig. 3c,d). S100A4 was not detectable in peripheral nerves (Fig. 3c,d), unlike other S-100 antibodies directed against different alpha and beta subtypes (Gonzalez-Martinez et al., 2003). Muscle fibres of skeletal muscle showed staining for S100A4 (Fig. 3e). Less intense and more localised was the S100A4 expression of smooth muscle cells in the urothelial mucosa (Fig. 3f). Also, the urothelium showed cytoplasmic positivity in occasional umbrella cells (Fig. 3f).

In skin (Fig. 4a), S100A4 staining was negative in keratinocytes, but showed strong positive staining in Langerhans cells (Fig.4b,d). Melanocytes did not express S100A4 (Fig. 4c).

In hypertrophic scar tissue (Fig. 5a), S100A4 showed variable cytoplasmic expression in dermal fibroblasts (Fig. 5d), often stronger in cells co-expressing smooth muscle actin (myofibroblasts; Fig. 5c). S100A4 staining was also seen in CD45+ leukocytes in this tissue (Fig. 5b). Stronger expression of S100A4 was seen in superficial fibromatosis (Fig. 6a,c,d). Also, here S100A4 expression mostly overlapped cells staining positive for smooth muscle actin (Fig. 6b).

Cultured synovial fibroblasts were predominantly negative for S100A4 (Fig. 7a). Smooth muscle actin was

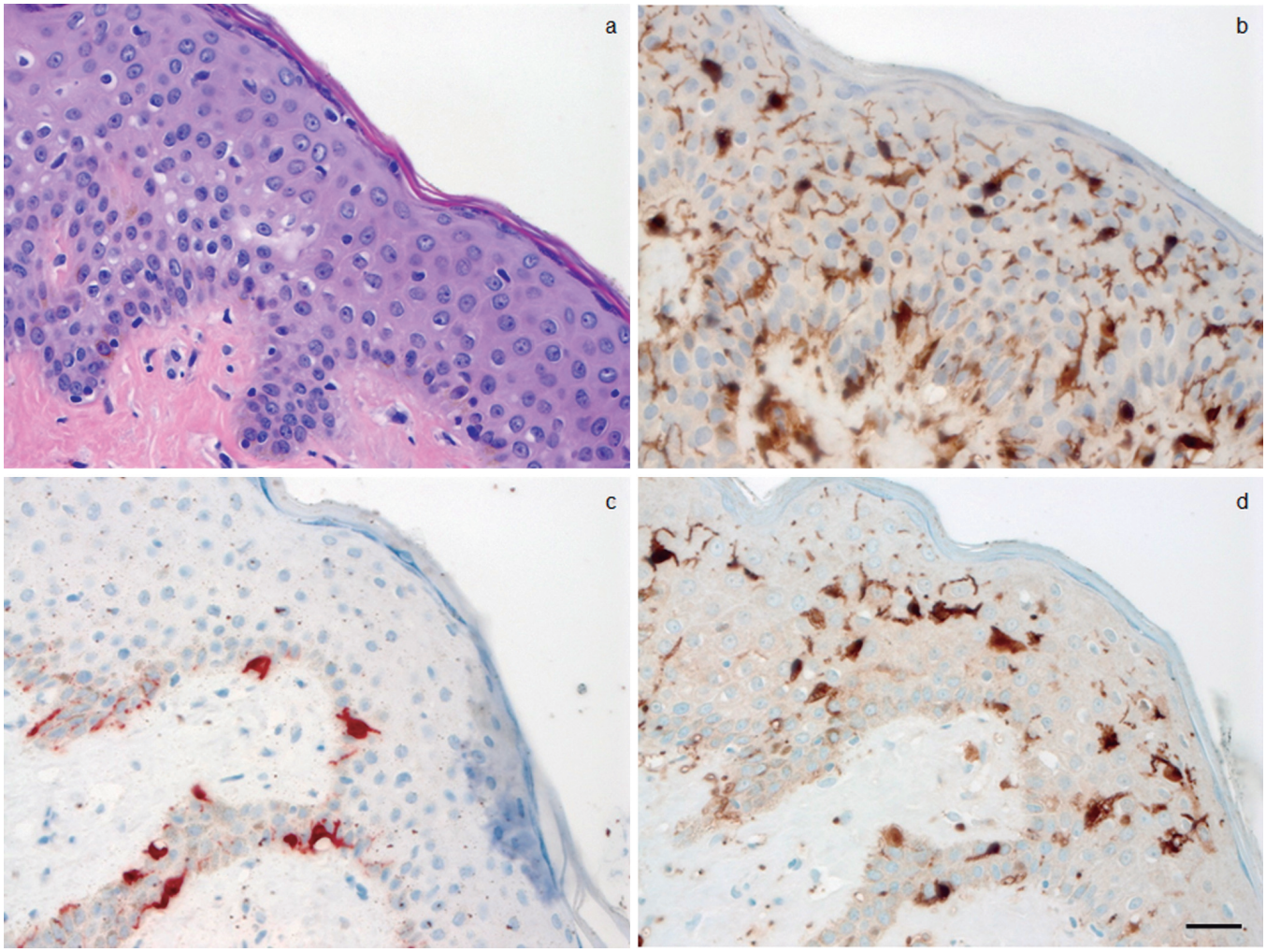

Fig. 4. a. Skin with slightly pigmented epidermis; hematoxylin and eosin stain. **b.** S100A4 staining mainly Langerhans histiocytes. **c.** MART-1/Tyrosinase staining melanocytes of the epidermis, negative in Langerhans cells. **d.** S100 (Dako Omnis) reacts strongly with human S100B and is positive in Langerhans cells. Scale bar: 50 μm. x 400.

rarely expressed by these fibroblasts (Fig. 7b). Accordingly, a positive immunohistochemical signal for S100A4 was only clearly detectable in the outer perimeter of 3D cultures of synovial fibroblasts (Fig. 7b), without staining for smooth muscle actin (Fig. 7d). Similarly, fibroblasts of tendon did mostly not or only weakly express S100A4 (Fig. 7e,f).

In the kidney (Fig. 8a,c), S100A4 was expressed in epithelial structures. The strongest and most uniform expression (nuclear and cytoplasmic) was seen in the loop of Henle (Fig. 8b). Also, many cells in the collecting duct expressed S100A4 (Fig. 8b). The distal tubules showed some nuclear and cytoplasmic positivity, more pronounced in the cortex of the kidney (Fig. 8d), with the most homogenous positivity seen in the macula densa (Fig. 8d).

Other investigated organs, including liver, breast, thyroid gland, pancreas, gallbladder, oesophagus, stomach, small intestine, skin and colon, did not express S100A4 in the epithelium (data not shown). The myofibroblast rich stromal cells of the prostate showed a diffuse predominantly moderate cytoplasmic expression of S100A4 (data not shown). The epithelial component in the prostate was negative for S100A4. Only a minority of cells of the uterine myometrium, made up of smooth muscle, showed a weak to moderate cytoplasmic expression of S100A4, the epithelium showed no reactivity for S100A4 (data not shown). The germinal epithelium of testis was negative for S100A4 (data not shown). The hormone secreting cells of the adrenal cortex were negative for S100A4, whereas the surrounding sustentacular cells were positive for

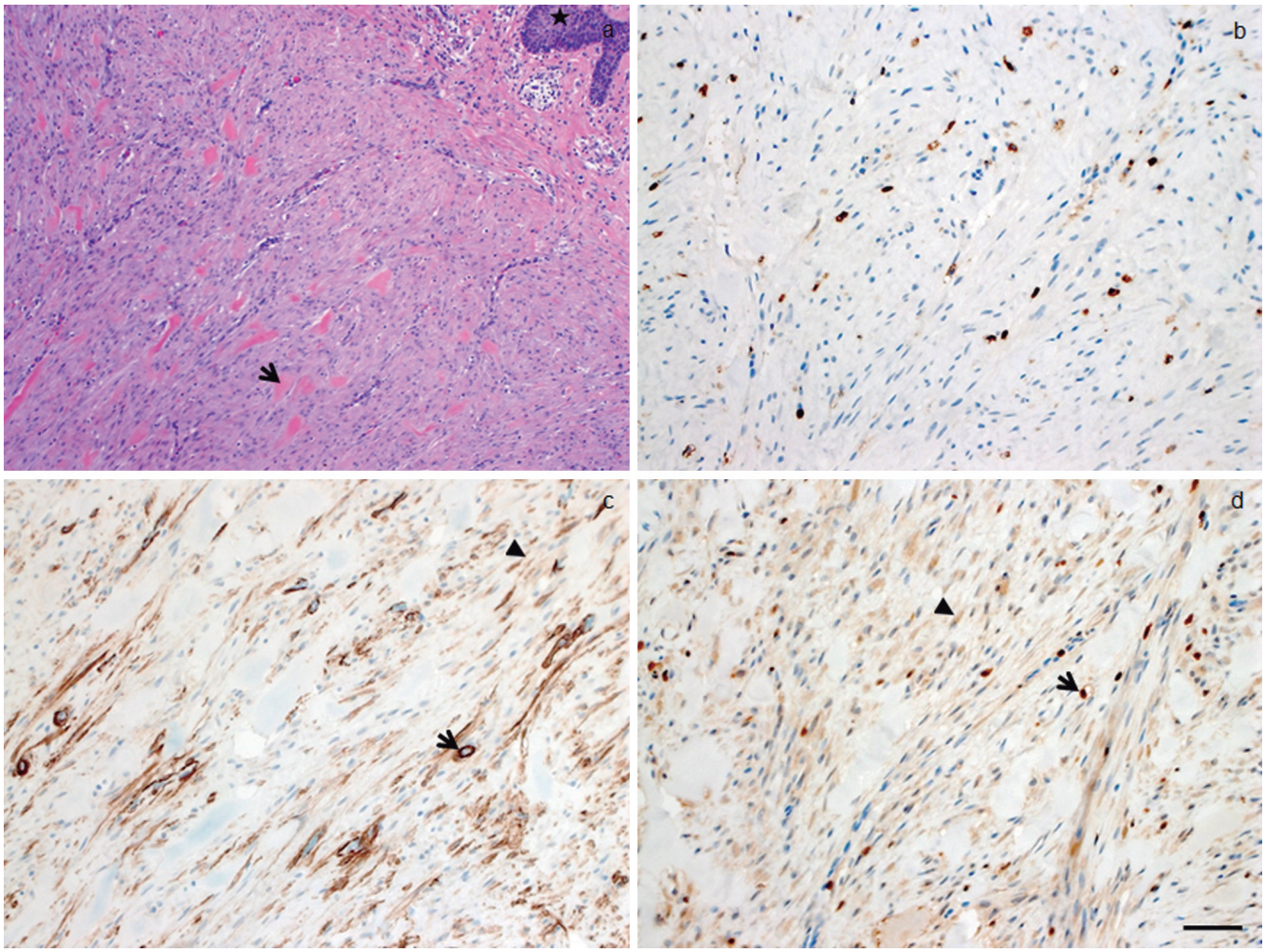

Fig. 5. a. Hypertrophic scar tissue in the dermis of the skin with focal epidermis (star), composed of fibroblasts/myofibroblasts (arrowhead), mononuclear inflammatory cells and keloid like fibrosis (arrow); hematoxylin and eosin stain. **b.** CD45 immunohistochemical staining (expressed in most leucocytes) highlighting the inflammatory cells in the scar tissue. **c.** Immunohistochemical staining for actin; expressed in myofibroblasts (arrowhead) and small blood vessels (arrow). **d.** S100A4 expressed in the cytoplasm of some fibroblasts/myofibroblasts (arrowhead). Strong nuclear and cytoplasmic expression in resident inflammatory cells and small blood vessels (arrow). Scale bar: 100 μm. a, x 100; b-d, x 200.

S100A4 (nuclear and cytoplasmic).

Astrocytes and oligodendrocytes in brain tissue did not express S100A4, but microglia were positive (data not shown).

In general, the strongest and most consistent nuclear and cytoplasmic S100A4 expression levels were seen in monocytes (Fig. 1d), macrophages and specialised histiocytes, including dendritic cells in lymph nodes (Fig. 2b,d), Langerhans cells of the skin (Fig. 4b,d), Kupffer cells of the liver (data not shown) and microglia of the brain (data not shown).

Discussion

To survey the distribution and extent of the expression of the calcium-binding protein FSP1/S100A4, we evaluated a broad range of organs and connective tissue incubated with a commonly used S100A4 antibody. We found that S100A4 is expressed in a wide range of cells, including cells of hematopoietic linage, connective tissue, including fibroblasts/myofibroblasts and even some epithelial cells of the kidney and bladder. The S100A4 antibody is therefore not specific for fibroblasts.

In many instances, FSP1/S100A4 was hardly detectable in fibroblasts in certain locations like tendon and synovium. In other locations, S100A4 was detectable in fibroblasts/myofibroblasts, especially in tissue with a high portion of smooth muscle actin positive myofibroblasts. This co-localization is likely linked to motility, a central function of S100A4, as was shown for histiocytic motility (Li et al., 2010). Consistent with a role in regulating cell motility, S100A4 has several reported cytoskeletal and scaffold protein targets including non-muscle tropomyosin 2, liprin-β1 and non-muscle myosin-IIA (Takenaga et al.,

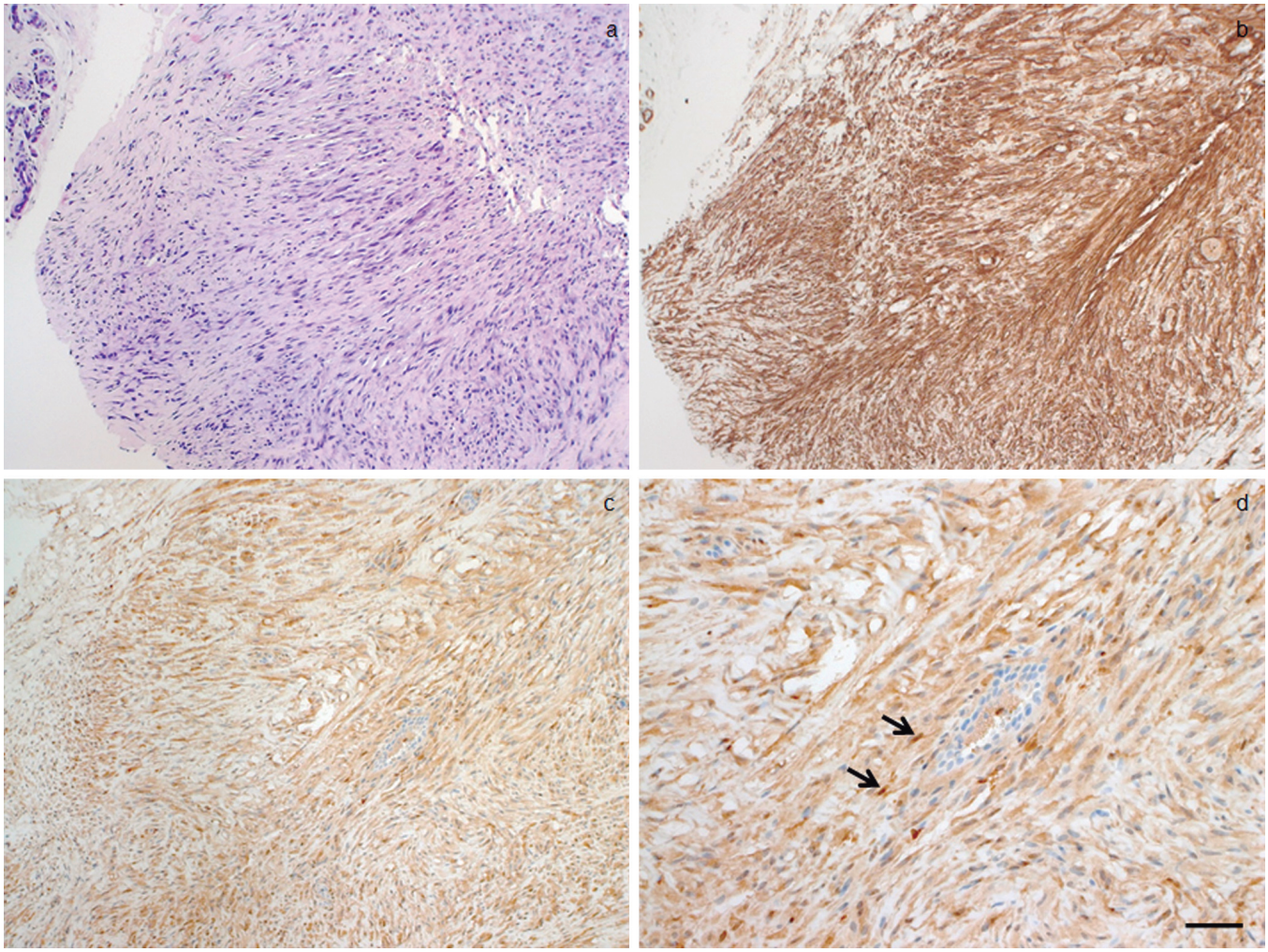

Fig. 6. a. Nodular proliferation of predominantly myofibroblasts in Dupuytren's contracture (Palmar Fibromatosis); Hematoxylin and eosin stain. **b.** Immunohistochemical staining for smooth muscle actin highlighting the predominant population of myofibroblasts. **c.** A moderate expression of S100A4 in the cytoplasm of most myofibroblasts. **d.** S100A4 staining at higher magnification (200x) also shows some vessel associated positive cells (arrows). Scale bar: 100 μm. a-c, x 100; d, x 200.

1994; Kriajevska et al., 2002; Ramagopal et al., 2013). Non-myosin IIA is a key cytoskeletal motor converting the chemical energy of adenosine triphosphate (ATP) into mechanical forces that mediate a static tension and contractility of actin filaments (De La Cruz and Ostap, 2004; Vicente-Manzanares et al., 2009). These contractile proteins are found in cardiac, skeletal and smooth muscle, in which sliding crossbridges that connect thick myosin filamentswith thin actin filaments provide the force needed. Also, in myofibroblasts non-muscle myosin type IIA acts as the molecular motor (Lecarpentier et al., 2021) and would explain the stronger expression of S100A4 in actin positive myofibroblasts compared to fibroblasts.

In the setting of chronic inflammation in the kidney, as used in the original description of EMT type 2, we are faced with the following problem. The kidney tissue is infiltrated by inflammatory cells and resident peritubular fibroblasts proliferate and transform to myofibroblasts (Picard et al., 2008). A discrimination of macrophages and fibroblasts based on S100A4 is therefore not possible.

Myofibroblasts are involved in the increased production of intercellular matrix and fibrosis, eventually leading to chronic renal failure. Additionally, tracing of tubular profiles (TEM) did not reveal gaps or defects in the tubular basement membrane and no cells were observed to cross the tubular basement membrane. The tubular cells accumulated lysosomal elements throughout the cell at day 4 after TGF-beta1 induction (beginning of autophagic process) but no positivity for S100A4 was observed in the tubules during the investigated time course. These findings suggest that upon damage, inflammatory cells migrate to the kidney, many of which express S100A4. Local fibroblasts proliferate and some transform to myofibroblasts that lead to fibrosis and depending on the severity and chronicity of the damage, to chronic renal failure (Le Hir et al., 2005; Picard et al., 2008).

Similarly, other researchers did not find evidence of epithelial mesenchymal transition. A paper published by Kriz et al. (Koesters et al., 2010) used a transgenic mouse model to induce TGF-beta1 in tubular epithelial cells after tetracycline application. TGF-beta1 has been proposed as a crucial factor to complete EMT (Gao et al., 2015). The investigators found that diffuse fibrosis is observed in the kidney already at day 2 after TGF-beta1 induction, preceding any tubular damage. Further they could show that resident fibroblasts in the peritubular spaces proliferate (Ki-67 positive) and that myofibroblasts develop from resident fibroblasts. After reappraising the originally published images during the emergence of the EMT type 2 theory (Strutz et al., 1995; Zeisberg et al., 2007), it is striking that the histological images depicted mostly show a nuclear S100A4 positivity in round cells with oval to kidney-bean shaped nuclei. This morphology is more consistent with monocytes/macrophages than spindle shaped fibroblasts/myofibroblasts. Also, our immunohistochemical evaluations mainly show a cytoplasmic rather than a

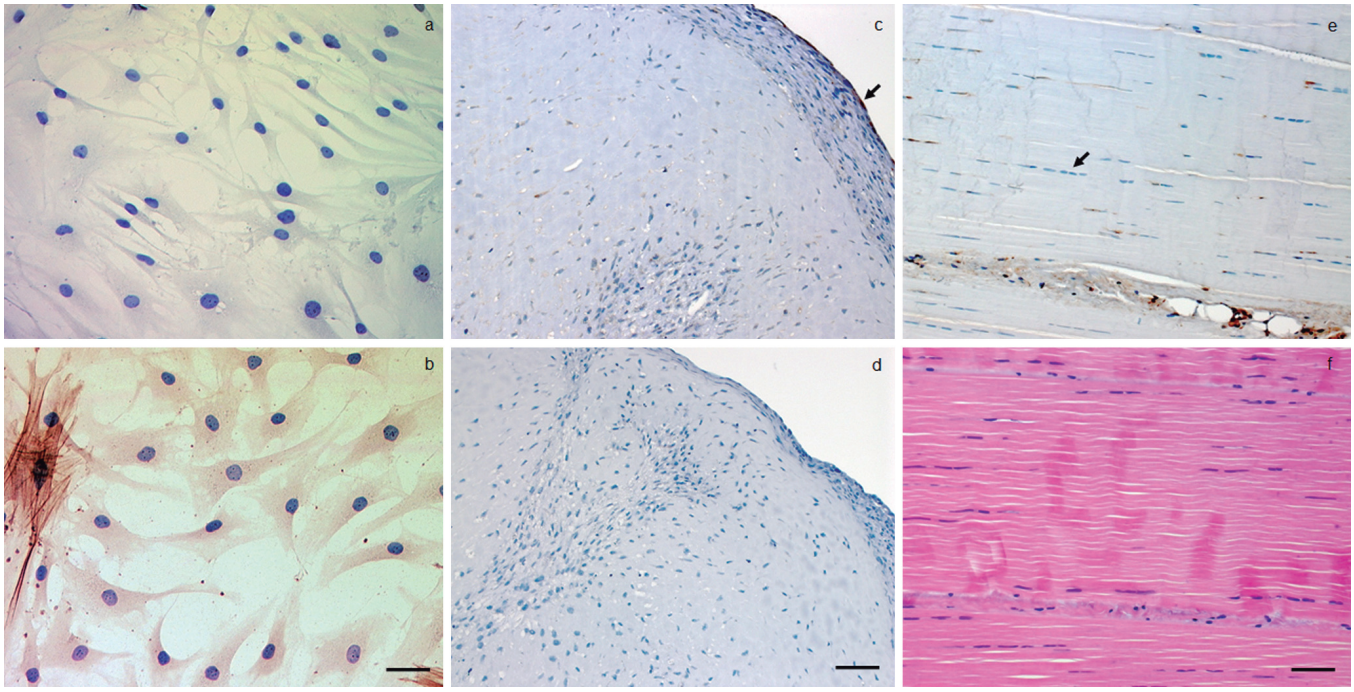

Fig. 7. a. Cultured synovial fibroblasts are predominantly negative for S100A4. **b.** Smooth muscle actin positive in a few myofibroblasts. **c.** 3D cultured synovial fibroblasts are predominantly negative for S100A4 with some positive cells in the perimeter (arrow). **d.** 3D cultured synovial fibroblasts negative for smooth muscle actin. **e.** Tendon fibroblasts (arrow) are predominantly negative for S100A4. **f.** Hematoxylin and eosin stain of a tendon. Scale bar: 100 μm. a, b, x 630; c-f, x 200.

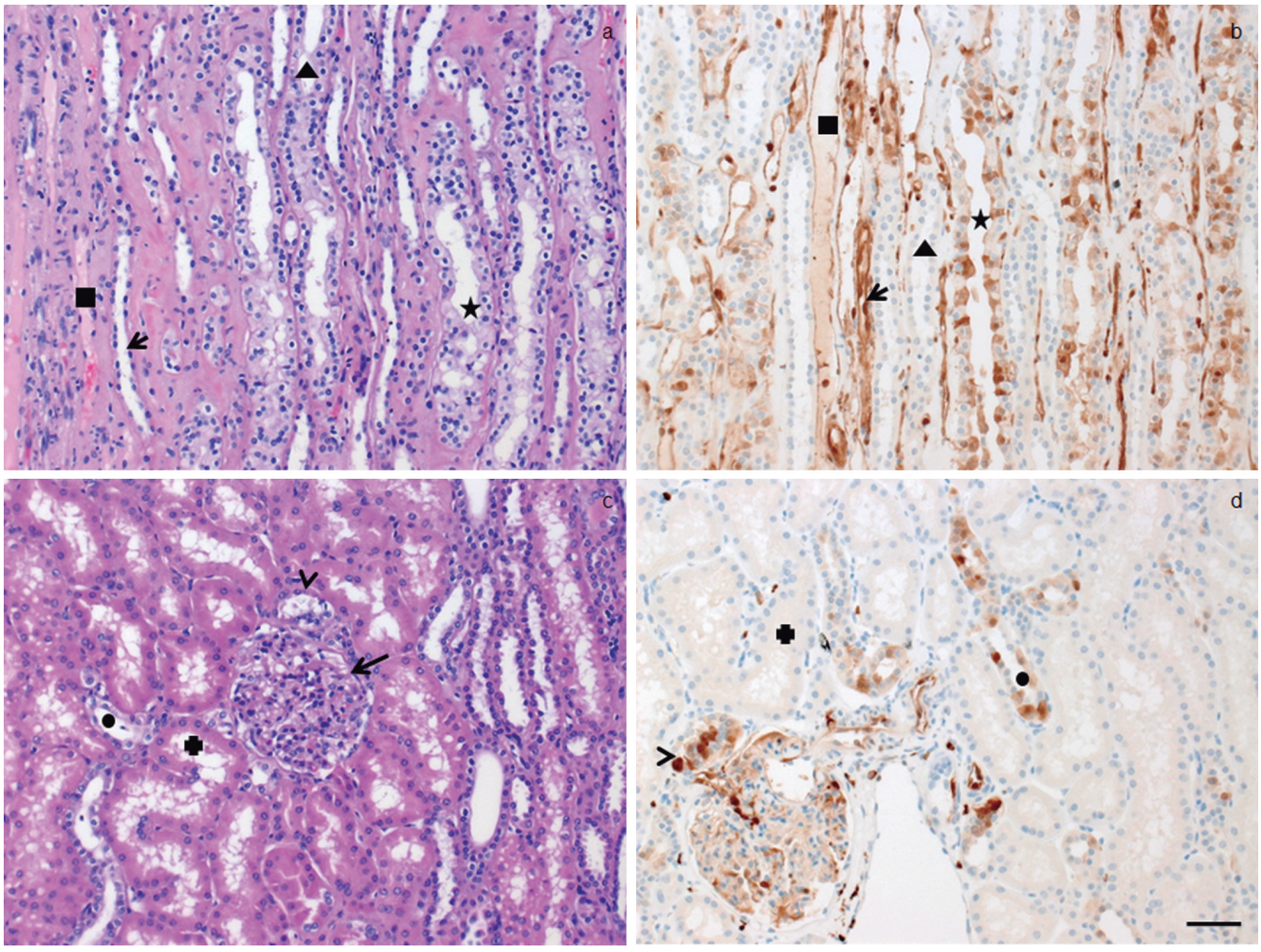

Fig. 8. a. Renal medulla made up of vasa rectae renis (square), collecting ducts (star), distal tubules (triangle) and loop of Henle (arrow). **b.** S100A4 staining of the renal medulla highlighting some positive cells (cytoplasmic and nuclear) in the collecting ducts (star), loop of Henle (arrow) and vasculature (square). Most of the cells in the distal tubules are negative (triangle). **c.** Renal cortex with a glomerulus (arrow), macula densa (arrowhead), proximal tubules (cross) and some distal tubules (circle9. **d.** S100A4 staining of the cortex with positivity in some cells of the distal tubules (circle), pronounced in the macula densa (arrowhead). The proximal tubules are negative for S100A4 (cross). Scale bar: 100 μm. x 200.

nuclear positivity in fibroblasts/myofibroblasts. In addition, under normal circumstances, S100A4 is expressed by many epithelial segments of the kidney without the epithelia being in an epithelial-mesenchymal transition. Therefore, an epithelial positivity for S100A4 cannot be equated to mesenchymal transition. Other regulatory and adaptive functions are linked to S100A4 positivity in the kidney. Researchers have shown that the absence of S100A4 profoundly delayed osmoadaptation and slowed cellular growth under hypertonic conditions (Rivard et al., 2007).

Taken together, the evidence for type 2 EMT is not very compelling. The S100A4 antibody labels many cells of the immune system, occasional epithelial cells as well as some fibroblasts/myofibroblasts. In the setting of chronic inflammation, as used in the original description of EMT type 2, a separation of inflammatory cells from fibroblast based on S100A4 positivity is therefore not possible. The insights gained by employing S100A4 to prove EMT type 2 consequently need to be interpreted with caution.

Compliance with ethical standards. The study was approved by the Ethics Committee Northwestern and Central Switzerland (EKNZ).

Funding. No funding was received for conducting this study.

Conflict of interest. The authors declare no conflict of interest.

Contributions. All authors contributed to the study conception and design. B.MF collected, analyzed and interpretated data, wrote the manuscript; A.H and M.B. collected data and critically reviewed the manuscript; E.C-R and C.O: collected, analyzed, interpreted data, and critically reviewed the manuscript; A.V: conceived and designed the project, collected, analyzed and interpretated data, wrote the manuscript and gave final approval. All authors read and approved the final manuscript.

References

Burns W.C. and Thomas M.C. (2010). The molecular mediators of type 2 epithelial to mesenchymal transition (EMT) and their role in renal pathophysiology. Expert Rev. Mol. Med. 12, e17.

De La Cruz E.M. and Ostap E.M. (2004). Relating biochemistry and function in the myosin superfamily. Curr. Opin. Cell. Biol. 16, 61-67.

Fei F., Qu J., Li C., Wang X., Li Y. and Zhang S. (2017). Role of metastasis-induced protein S100A4 in human non-tumor pathophysiologies. Cell. Biosci. 7, 64.

Gao J., Yan Q., Wang J., Liu S. and Yang X. (2015). Epithelial-to-mesenchymal transition induced by TGF-β1 is mediated by AP1-dependent EpCAM expression in MCF-7 cells. J. Cell. Physiol. 230, 775-782.

Gonzalez-Martinez T., Perez-Piñera P., Díaz-Esnal B. and Vega J.A. (2003). S-100 proteins in the human peripheral nervous system. Microsc. Res. Tech. 60, 633-638.

Hertig A., Verine J., Mougenot B., Jouanneau C., Ouali N., Sebe P., Glotz D., Ancel P.Y., Rondeau E. and Xu-Dubois Y.C. (2006). Risk factors for early epithelial to mesenchymal transition in renal grafts. Am. J. Transplant. 6, 2937-2946.

Kalluri R. and Weinberg R.A. (2009). The basics of epithelial-mesenchymal transition. J. Clin. Invest. 119, 1420-1428.

Kiener H.P., Watts G.F., Cui Y., Wright J., Thornhill T.S., Sköld M., Behar S.M., Niederreiter B., Lu J., Cernadas M., Coyle A.J., Sims G.P., Smolen J., Warman M.L., Brenner M.B. and Lee D.M. (2010). Synovial fibroblasts self-direct multicellular lining architecture and synthetic function in three-dimensional organ culture. Arthritis Rheum. 62, 742-752.

Koesters R., Kaissling B., Lehir M., Picard N., Theilig F., Gebhardt R., Glick A.B., Hahnel B., Hosser H., Grone H.J. and Kriz W. (2010). Tubular overexpression of transforming growth factor-β1 induces autophagy and fibrosis but not mesenchymal transition of renal epithelial cells. Am. J. Pathol. 177, 632-643.

Kriajevska M., Fischer-Larsen M., Moertz E., Vorm O., Tulchinsky E., Grigorian M., Ambartsumian N. and Lukanidin E. (2002). Liprin β1, a member of the family of LAR transmembrane tyrosine phosphatase-interacting proteins, is a new target for the metastasis-associated protein S100A4 (Mts1). J. Biol. Chem. 277, 5229-5235.

Kutlu T. and Alcigir G. (2019). Comparison of renal lesions in cats and dogs using pathomorphological and immunohistochemical methods. Biotech. Histochem. 94, 126-133.

Le Hir M., Hegyi I., Cueni-Loffing D., Loffing J. and Kaissling B. (2005). Characterization of renal interstitial fibroblast-specific protein 1/S100A4-positive cells in healthy and inflamed rodent kidneys. Histochem. Cell Biol. 123, 335-346.

Lecarpentier Y., Claes V., Hebert J.L., Schussler O. and Vallee A. (2021). Mechanical and thermodynamic properties of non-muscle contractile tissues: The myofibroblast and the molecular motor non-muscle myosin type IIA. Int. J. Mol. Sci. 22.

Li Z.H., Dulyaninova N.G., House R.P., Almo S.C. and Bresnick A.R. (2010). S100A4 regulates macrophage chemotaxis. Mol. Biol. Cell 21, 2598-2610.

Li Z., Li Y., Liu S. and Qin Z. (2020). Extracellular S100A4 as a key player in fibrotic diseases. J. Cell. Mol. Med. 24, 5973-5983.

Orre L.M., Panizza E., Kaminskyy V.O., Vernet E., Graslund T., Zhivotovsky B. and Lehtio J. (2013). S100A4 interacts with p53 in the nucleus and promotes p53 degradation. Oncogene 32, 5531-5540.

Picard N., Baum O., Vogetseder A., Kaissling B. and Le Hir M. (2008). Origin of renal myofibroblasts in the model of unilateral ureter obstruction in the rat. Histochem. Cell. Biol. 130, 141-155.

Ramagopal U.A., Dulyaninova N.G., Varney K.M., Wilder P.T., Nallamsetty S., Brenowitz M., Weber D.J., Almo S.C. and Bresnick A.R. (2013). Structure of the S100A4/myosin-IIA complex. BMC Struct. Biol. 13, 31.

Rivard C.J., Brown L.M., Almeida N.E., Maunsbach A.B., Pihakaski-Maunsbach K., Andres-Hernando A., Capasso J.M. and Berl T. (2007). Expression of the calcium-binding protein S100A4 is markedly up-regulated by osmotic stress and is involved in the renal osmoadaptive response. J. Biol. Chem. 282, 6644-6652.

Saitoh M. (2018). Involvement of partial EMT in cancer progression. J. Biochem. 164, 257-264.

Sherbet G.V. (2009). Metastasis promoter S100A4 is a potentially valuable molecular target for cancer therapy. Cancer Lett. 280, 15-30.

Strutz F., Okada H., Lo C.W., Danoff T., Carone R.L., Tomaszewski J.E. and Neilson E.G. (1995). Identification and characterization of a fibroblast marker: FSP1. J. Cell Biol. 130, 393-405.

Takenaga K., Nakamura Y., Sakiyama S., Hasegawa Y., Sato K. and Endo H. (1994). Binding of pEL98 protein, an S100-related calcium-binding protein, to nonmuscle tropomyosin. J. Cell Biol. 124, 757-768.

Thiery J.P., Acloque H., Huang R.Y. and Nieto M.A. (2009). Epithelial-mesenchymal transitions in development and disease. Cell 139, 871-890.

Vicente-Manzanares M., Ma X., Adelstein R.S. and Horwitz A.R. (2009). Non-muscle myosin II takes centre stage in cell adhesion and migration. Nat. Rev. Mol. Cell. Biol. 10, 778-790.

Zeisberg M., Yang C., Martino M., Duncan M.B., Rieder F., Tanjore H. and Kalluri R. (2007). Fibroblasts derive from hepatocytes in liver fibrosis via epithelial to mesenchymal transition. J. Biol. Chem. 282, 23337-23347.

Accepted April 13, 2023